TNF-α–induced apoptosis in the absence of NF-κB activation, and that NF-κB–mediated inhibition on JNK activation is important for cell survival (*21–24*). Here we show that, in wild-type DT40 cells, high-level production of AIB1 suppresses the phosphorylation of JNK and c-Jun, the main physiological substrate of the JNK kinase, in response to cellular stress such as serum deprivation or UV irradiation. In contrast, loss of AIB1 leads to inhibition of activation of the Akt/p65 signaling pathway and suppresses DNA synthesis.

Finally, we found that AIB1 enhances the induction of phosphorylation of histone H3 at serine 10 but not the acetylation of histone H3 at lysine 9 or lysine 14 in response to UV stress. Phosphorylation of histones provides motifs for the recruitments of chromatin modifying or remodelling complexes, including coactivators which are linked to cellular processes such as transcription, DNA replication, DNA repair and apoptosis in the stress response (*25*, *26*). Because AIB1 enhances the induction of phosphorylation of histone H3 at serine 10, it plays a critical role as a transcriptional modifier that is recruited for chromatin remodelling in response to cellular stresses. These results indicate that changes in AIB1 production may determine cell fate in association with the balances between the Akt/p65 and JNK/c-Jun signaling pathways in cellular stress responses.

EXPERIMENTAL PROCEDURES

Cell Culture—DT40 cell lines were maintained in RPMI 1640 (Nikkenseibutsu) medium supplemented with 10% fetal calf serum (FCS; Gibco BRL) and 1% chicken serum (JRH Bioscience) at 39.5°C in a humidified atmosphere with 5% CO_2. Cell density was maintained at 0.1–1.0/10^6 ml by splitting the culture daily.

Construction of Targeting and Expression Vectors—A chicken AIB1 (*GdAIB1*) partial cDNA fragment from the bHLH/PAS domain was amplified from chicken brain cDNA by RT-PCR with primers (5′-aaggaaaaactatttccagtgagatgatgttc-3′, 5′-cgaattgtatcctaaagccaggtctcagg-3′). We then used 5′ and 3′ RACE on chicken brain cDNA to isolate the entire open reading frame of *GdAIB1*. To construct the *GdAIB1* expression vector, chicken *AIB1* cDNA was inserted into an expression vector containing the chicken β-actin promoter. We then isolated 6.5 kb of the partial chicken genomic *GdAIB1* locus from DT40 genomic DNA by long-range PCR. Chicken *AIB1* targeting constructs were made by replacing the genomic sequence containing the sequence encoding amino acids 122 to 156 with hygromycin or histidinol selection marker cassettes.

Generation of AIB1 -/- Clones—10^7 DT40 cells were suspended in 0.5 ml PBS containing 30 μg of linearized plasmid for the transfection and electroporated with a Gene Pulser apparatus (BioRad) at 550 V and 25 μF. Following electroporation, cells were transferred into 20 ml fresh medium and incubated for 24 h. Cells were then resuspended in 80 ml medium containing hygromycin (2.5 mg/ml, Calbiochem) or L-histidinol (1 mg/ml, Calbiochem) and divided into four 96-well plates. After 7 to 10 days, drug-resistant colonies were selected. Disruption of the gene was confirmed by Southern blot analysis of genomic DNA.

Cell Cycle Analysis—A total of of 2×10^5 cells were treated with 5-bromodeoxyuridine (BrdU; 10 μM, Sigma) for 10 min and the subconfluent cells harvested. After fixation with 70% ethanol, the cells were incubated overnight at −20°C. The next day, cells were collected and resuspended in 2 N HCl with 0.5% Triton X-100 for 30 min at room temperature; this was followed by neutralization with 0.1 M $Na_2B_4O_7$. Cells were then collected and incubated with anti-BrdU antibody (Becton-Dickinson) for 30 min in the dark at room temperature. The cells were washed with PBS and stained with FITC-labeled goat anti-mouse Abs (Jackson) for 30 min at room temperature in the dark. The cells were resuspended in PBS containing propidium iodide (5 μg/ml, Sigma). The filtered cells were analyzed by fluorescence-activated cell sorter (FACScan, Becton-Dickinson). The distribution of cells in each phase of the cell cycle was determined by using Cell Quest software (Becton-Dickinson).

TUNEL Assay—DT40 cells were harvested at the designated time points and fixed in 70% ethanol in PBS. The fixed cells were then incubated for 30 min at 4°C and permeabilized with 0.2% Triton X-100 in PBS for 5 min. For apoptosis analysis, the cells were examined by the TUNEL technique, as described in the instructions supplied with the apoptosis detection system (Takara). Localized green fluorescent apoptotic cells were detected by fluorescence microscopy. The percentage of FITC-positive cells in the apoptotic fraction was determined in a fluorescence-activated cell sorter (Becton Dickinson).

Western Blot Analysis—Cells were lysed in lysis buffer (150 mM NaCl, 50 mM Tris-HCl at pH 7.5, and 1% NP-40) supplemented with protease inhibitors, aprotinin (1 μg/ml), and leupeptin (2 μg/ml). Lysates were centrifuged to clear cell debris, and then 30 μg of the total protein were size-fractionated by SDS-PAGE gel (7.5% to 15%). After electrophoresis, proteins were transferred to PVDF membranes (BioRad), blocked in PBS containing 0.2% Tween 20 and 3% bovine serum albumin, and probed with first antibody in PBS containing 0.2% Tween 20 and 1% bovine serum albumin. Detection of the immune signal was performed with the chemiluminescence detection system (Amersham Biosciences) and then quantified using densitometry (Molecular Dynamics).

Antibodies—The amino-terminal portion of chicken AIB1 (amino acids 1 to 250) was expressed in *E. coli* as a histidine tagged fusion protein and purified by affinity chromatography using Ni-agarose (Qiagen). The purified protein was then injected into rabbits to prepare specific antiserum. Rabbit antibodies of anti-phospho-Akt, anti-Akt, anti-phospho-p65, anti-p65, anti-phospho-JNK, anti-JNK, anti-phospho-c-Jun, anti-c-Jun, anti-phospho-p38, and anti-phospho-p44/42 ERK1/2 were purchased from Cell Signaling Technology. Mouse antibodies of anti-p38 and anti-ERK1 were purchased from BD Bioscience. Rabbit anti-histone H3 phosphorylated at Ser10 or Ser28 and rabbit anti-histone H3 acetylated at Lys9 or Lys14 antibodies were purchased from Upstate Biotechnology.

Immunoprecipitations and In Vitro Akt Kinase Assay—Cells were disrupted with cold RIPA buffer (50 mM Tris-HCl, pH 8.0, 150 mM NaCl, 1% NP-40, 0.5% DOC, and 0.1% SDS) containing protease inhibitors, aprotinin (1 μg/ml) and leupeptin (2 μg/ml). Approximately 200 μg of protein lysate was incubated with anti-chicken AIB1

antibody and anti-Akt antibody overnight at 4°C with end-over-end rotation, followed by an additional 2 h of incubation with protein A sepharose beads (Amersham Biosciences). The beads were then washed three times with cold RIPA buffer before being boiled in SDS-PAGE sample buffer. *In vitro* Akt kinase assay was performed for 30 min at 30°C in 40 μl of reaction volume containing 30 μl of immunoprecipitates in kinase buffer with 200 μM ATP. GSK-3 fusion protein (Cell Signaling Technology) was used as a substrate for Akt kinase activity. The reactions were terminated with 20 μl of SDS sample buffer and subjected to Western blotting using anti-phospho-GSK antibody (Cell Signaling Technology).

Northern Blot Analysis—Total RNA was isolated with Trizol reagent (Invitrogen). For generation of each probe, 1 μg of total RNA was used in reverse transcription reactions, as described by the manufacturer. The resulting total cDNA was then used in the PCR to estimate mRNA levels. The mRNA level of GAPDH was used as internal control. PCR was carried out with Taq polymerase, and the conditions were as follows: pre-denaturing at 94°C for 3 min, then 30 cycles of 94°C for 30 s, 60°C for 30 s, and 72°C for 30 s. The oligonucleotide primers used to generate these probes were as follows: AIB1 (GenBank accession number: XM417385), 5′-attacctgcattcagagaagaat-3′ and 5′-tcttctctcattgtctacacaa-3′; chicken cyclin D1 (U40844), 5′-tttacaccgacaactccatc-3′ and 5′-gtgataggaaatgtgtgagg-3′; chicken cyclin D2 (U28980), 5′-ccatcaatgatagcaactgg-3′ and 5′-aaaataaaaggggtgggag-3′; chicken cyclin E (U28981), 5′-cttcaccgctaccaattctg-3′ and 5′-caaactggtgcaactttggt-3′; chicken E2F1 (X89245), 5′-ggatccccggcagaggggca-3′ and 5′-ctccaggacattggtgatgt-3′; GAPDH (NM204305), 5′-accactgtccatgccatcac-3′ and 5′-tccacaacacggttgctgta-3′. Each total RNA (30 μg) was run on a 1.0% formaldehyde gel and transferred to a Hybond N+ nylon membrane (Amersham) using a Turbo blotter system (Schleicher & Schuell). DNA probes were labeled with [α-^{32}P] dCTP (Amersham Biosciences) using a random labeling kit (Takara). The membrane was hybridized with labeled DNA probes by QuikHyb hybridization (Stratagene) at 65°C for 2 h and then developed for autoradiography.

Histone Extraction—Cells were centrifuged, the medium discarded and the cells washed twice with PBS (pH 7.4). The cells were suspended in 5 to 10 volumes of lysis buffer (10 mM HEPES, pH 7.5, 1.5 mM $MgCl_2$, 10 mM KCl, 0.5 mM DTT and 1.5 mM PMSF). The samples were incubated on ice for 30 min and centrifuged at 1,000 × *g* for 10 min at 4°C. The supernatant was discarded, and the histones in the pellets were extracted by 0.2 M HCl solution. The samples were centrifuged at 12,000 × *g* for 10 min at 4°C after incubation on ice for 30 min. The histones were then precipitated from acid solution with 5 volumes of cold acetone.

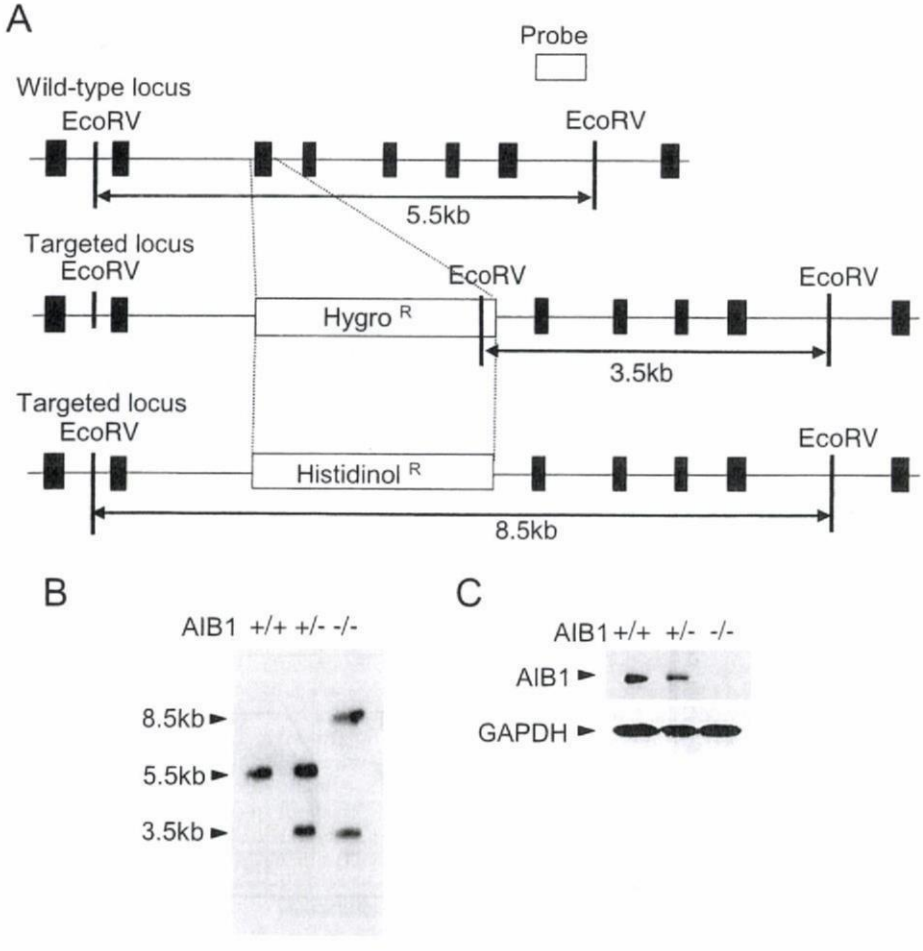

Fig. 1. **Generation of AIB1-knockout DT40 cells.** (A) Schematic representation of the targeting vectors. The configuration of the wild-type allele is shown at the top. In the targeting vectors, the exon encoding the Per-Arnt-Sim (PAS) domain is replaced by a hygromycin or histidinol resistance gene cassette. Solid boxes indicate positions of exons deduced from the cDNA sequence. The location of the external probe used to confirm correct targeted events and the location of the relevant *EcoRV* recognition sites are indicated. (B) Southern blot analysis of targeted integration. A DT40 cell in which one *AIB1* allele had been disrupted by the targeting construct of AIB1-hygromycin, was transfected with the second construct of AIB1-Histidinol. Genomic DNAs from untransfected DT40 cells (+/+) and doubly resistant clones (–/–) were digested with *EcoRV* and hybridized with the probe shown in (A). (C) Western blot analysis of wild-type, AIB1$^{+/-}$ and AIB1$^{-/-}$ DT40 cells. GAPDH protein was detected as an internal control.

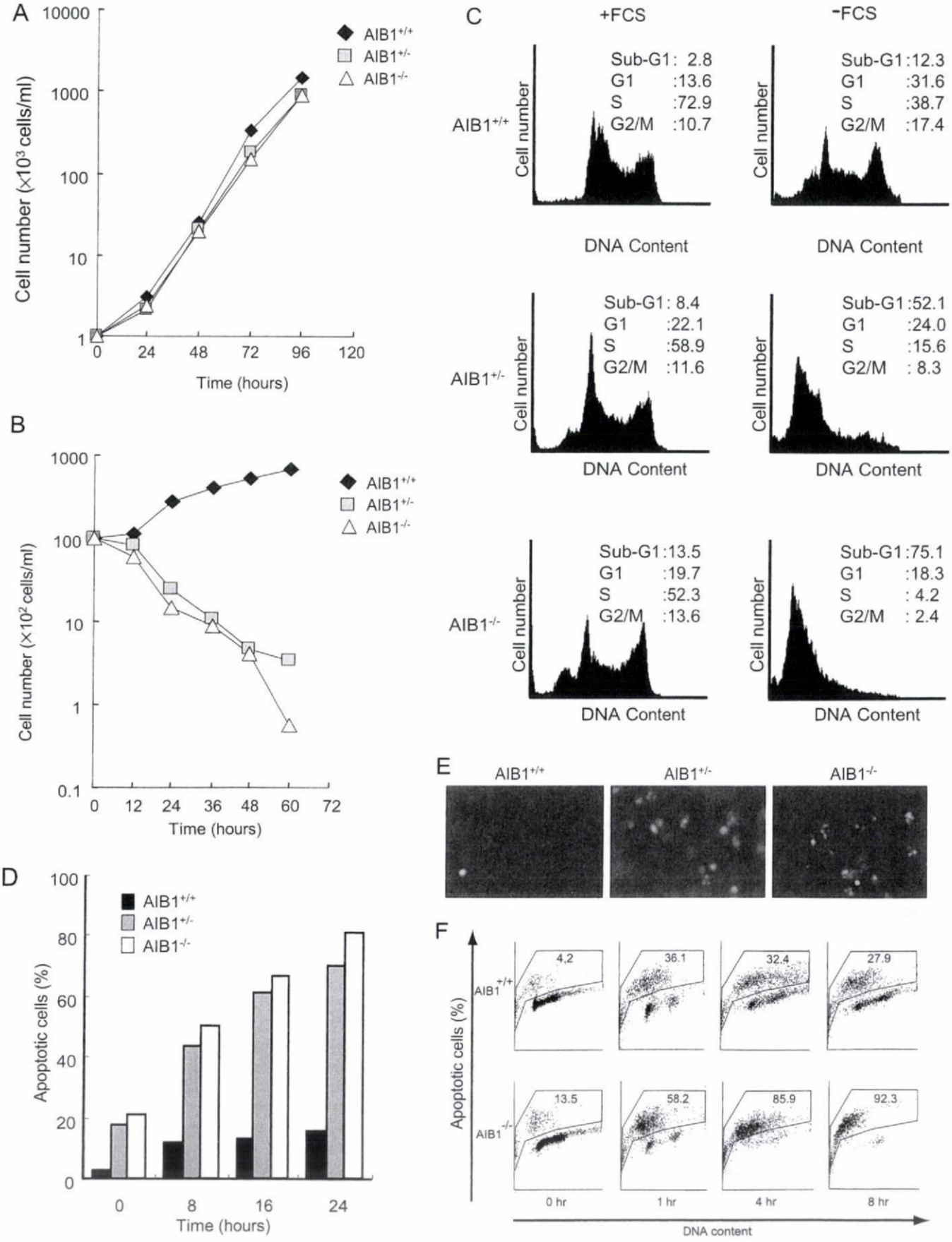
A
Cell number (×10³ cells/ml)
Time (hours)
AIB1+/+
AIB1+/-
AIB1-/-
B
Cell number (×10² cells/ml)
Time (hours)
C
+FCS
-FCS
Sub-G1: 2.8
G1 :13.6
S :72.9
G2/M :10.7
Sub-G1:12.3
G1 :31.6
S :38.7
G2/M :17.4
Sub-G1: 8.4
G1 :22.1
S :58.9
G2/M :11.6
Sub-G1:52.1
G1 :24.0
S :15.6
G2/M : 8.3
Sub-G1:13.5
G1 :19.7
S :52.3
G2/M :13.6
Sub-G1:75.1
G1 :18.3
S : 4.2
G2/M : 2.4
Cell number
DNA Content
D
Apoptotic cells (%)
Time (hours)
E
F
4.2
36.1
32.4
27.9
13.5
58.2
85.9
92.3
0 hr
1 hr
4 hr
8 hr
DNA content

RESULTS

Generation of AIB1-Knockout DT40 Cells—To investigate the biological function of AIB1 in the signal transduction pathways triggered by cellular stress, we generated a model for the elimination of AIB1 production by using DT40 B-lymphocytes that constitutively express high levels of *c-myc* as a result of transformation by an avian leukosis virus (*27*). Because of their high rate of homologous recombination in vertebrate cells, DT40 cell lines have also been used as models for establishing strategies to identify genes that encode undiscovered components of a process or a pathway (*28*). We previously reported the cloning of a chicken homologue of AIB1 that exhibits 74.4% amino acid sequence similarity to human AIB1 (*29*). A full-length transcript of the gene encoding chicken AIB1 was isolated and found to encode a 1,399–amino acid protein. An AIB1 deletion construct was generated (Fig. 1A) and a portion of the AIB1 genomic locus was replaced with a hygromycin resistance gene and a histidinol resistance gene. The targeted homologous recombination in DT40 cells was confirmed by Southern blot analysis of genomic DNA (Fig. 1B). The deleted region encoded amino acid residues 122 to 156, including the PAS domain. AIB1-knockout DT40 cells were detected by Western blot analysis using anti-AIB1 antibody (Fig. 1C).

AIB1 Promotes Cell Survival in Response to Cellular Stress in DT40 Cells—To determine the roles of AIB1 in mechanisms mediated by exposure to cellular stress in cancer cells, we examined whether loss of AIB1 was associated with changes in the regulatory mechanism of cell proliferation and cell death. Under standard culture conditions, we detected no significant difference in the rates of cell proliferation of wild-type and AIB1-knockout DT40 cells (Fig. 2A). However, AIB1-knockout cells were more susceptible to cell death than were wild-type cells in response to cellular stresses such as serum starvation. Usually, DT40 cells were maintained in medium with 10% FCS and 1% chicken serum. After deprivation of FCS, survival number of AIB1-knockout cells rapidly decreased in contrast with wild type cell (Fig. 2B). The heterozygote also manifested considerable decrease in cell number, suggesting that gene dosage of AIB1 is crucial for cell survival under serum starvation (Fig. 2B). FACS analysis revealed that 75.1% of the AIB1-knockout cells were in the sub-G1 fraction (reflecting cell death), as compared to 12.3% for the wild-type cells under serum starvation (Fig. 2C). In contrast, the S-fraction (indicating DNA synthesis) was greater in wild-type cells than in AIB1-knockout cells (Fig. 2C). In order to confirm that these cell death were apoptosis, we carried out TUNEL analysis. When cells were stained by the TUNEL after deprivation of FCS, the double-stained cells (reflecting apoptosis) increased much more in $AIB1^{+/-}$ and $AIB1^{-/-}$ DT40 cells than in wild-type DT40 cells (Fig. 2, D, E). We observed similar results in the responses to not only serum starvation but also other forms of cellular stress, such as UV irradiation (10 J/m^2) (Fig. 2F) and culture at low temperature (data not shown). These results revealed that loss of AIB1 increased apoptosis in AIB1-knockout cells under cellular stress conditions.

Deletion of AIB1 Enhances Stress-Induced JNK/c-Jun Activation and Prevents Akt/p65 Activation—Signal cascades in response to cell survival have been linked to cancer and inflammatory disease. Previous studies have shown that cellular responses are regulated by the signaling pathways that lie downstream of the Ras induced by cross talk between the Raf-MER-ERK and PI3K-Akt pathways in breast cancer cells (*21*, *22*). Moreover, the PI3K/Akt/NF-κB pathway plays an important role in preventing cells from undergoing apoptosis and contributes to the pathogenesis of malignancy (*23*). Recently, cell proliferation and survival were reported to require activation of the PI3K/Akt pathway, which has been implicated in the control of Myc protein stability (*24*). The most recent study in transgenic mice also implicated overexpression of the *AIB1* gene in the etiology of breast cancer (*15*). However, these findings and our results in Fig. 2 raise the possibility that increased AIB1 production serves to promote cell survival through the PI3K/Akt pathway in response to cellular stress. Cell survival in response to stressful stimuli has been implicated in the activation of many signal transduction pathways, such as the p38 mitogen-activated protein kinase (MAPK) pathway, the stress-activated JNK pathway, and the PI3K/Akt pathway (*30–32*). Therefore, we investigated how signal pathways might be involved in AIB1-mediated cell survival in response to cellular stress. For Western blot analysis, wild-type and AIB1-knockout DT40 cells were cultured under normal conditions or cellular stress conditions. At first, stressful stimuli such as serum starvation or UV irradiation induced phosphorylation of NF-κB subunit p65 and Akt in wild-type DT40 cells (Fig. 3A). In contrast, phosphorylation of p65 and Akt were abolished in AIB1-knockout cells (Fig. 3A). To confirm the Akt activation under stress conditions, Akt activity was detected by an

Fig. 2. **AIB1 promotes cell survival in response to serum starvation and UV irradiation.** (A) Growth curves of wild-type, $AIB1^{+/-}$ and $AIB1^{-/-}$ DT40 cells under standard conditions. Cells were cultured in RPM1640 medium supplemented with 10% fetal calf serum (FCS) and 1% chicken serum at 39.5°C. Representative growth curves correspond to the indicated cell cultures. The number of cells was counted every 24 h by FACS with polybeads as the internal standard. Each experiment was conducted three times, and each time point was determined in triplicate. (B) AIB1 was required for cell survival under serum-starved conditions. Cells were cultured at 39.5°C in fresh RPM1640 medium supplemented with 1% chicken serum, after being maintained continuously with 10% FCS and 1% chicken serum. The number of cells was counted every 12 h. (C) Cell cycle analyses of wild-type, $AIB1^{+/-}$, and $AIB1^{-/-}$ DT40 cells in the presence or absence of FCS over 24 h. The DNA content of the cultured cells was examined by propidium iodide staining. The populations of the sub-G1, G1, S, and G2/M fractions are indicated by percentages. (D) Wild-type DT40 cells were inhibited from undergoing apoptosis under serum starvation, as measured by TUNEL analysis. Cells were cultured in the absence of FCS for the periods indicated. The cells were then stained for TUNEL analysis. Double-stained cells were counted as apoptotic and are shown as the percentages in three independent experiments. (E) DNA breaks, characteristic of apoptosis, were detected under fluorescent microscope by TUNEL analysis. Cells were harvested after being cultured for 8 h in the absence of FCS. (F) DNA replication was induced in wild-type DT40 cells under the stimulation of UV-irradiation, as measured by TUNEL analysis. After UV-irradiation (10 J/m^2) the cells were cultured for the periods indicated and then stained for TUNEL analysis. Double-stained cells were counted as apoptotic and are shown as percentages from three independent experiments.

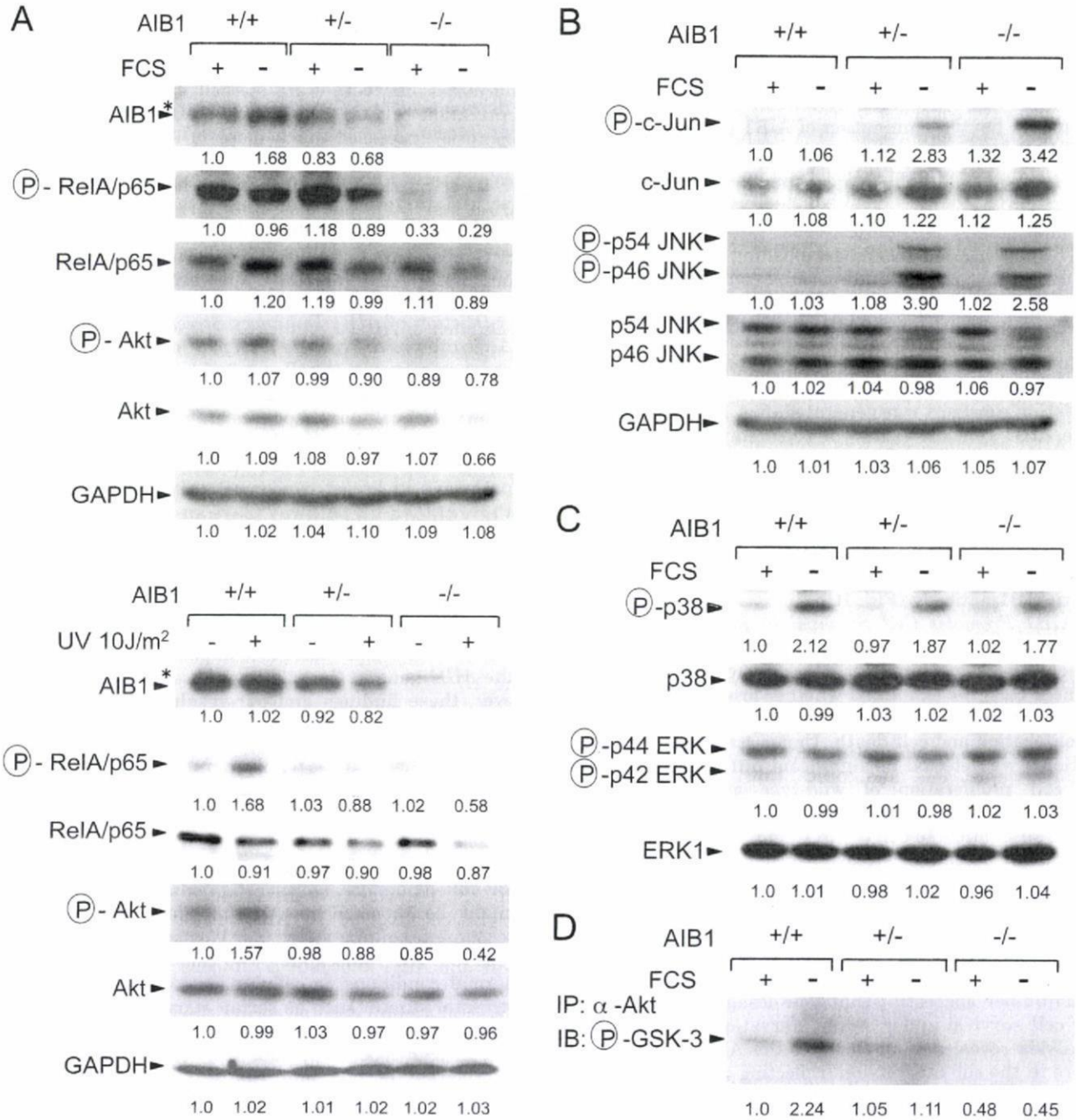

Fig. 3. **Activation of AIB1 triggers Akt survival pathway and blocks JNK-mediated cell death.** (A) Serum starvation and UV irradiation of wild-type DT40 cells induced Akt and p65 phosphorylation. The levels of production of proteins and phosphoproteins in the Akt/NF-κB cell-survival pathway were indicated by immunoblot analysis using 30 μg cell extracts prepared from wild-type, AIB1$^{+/-}$, or AIB1$^{-/-}$ DT40 cells cultured for 8 h in the presetnce or absence of FCS, with or without stimulation of UV-irradiation (10 J/m^2). The "P" in the circles indicates phosphorylation. The asterisk indicates that AIB1 antibody cross-reacted with the unspecific cytoplasmic protein. (B) Phosphorylation of JNK and c-Jun were induced by serum starvation in AIB1-knockout cells. The levels of production of protein and phosphoprotein in the JNK-mediated apoptosis pathway are indicated as shown in (A). (C) The presence of AIB1 protein did not affect the activation of the ERK or p38 MAPK pathways. (D) Serum starvation of wild-type DT40 cells induced Akt kinase activity. *In vitro* kinase assay was performed with immunoprecipitated Akt. Akt kinase activity is indicated by immunoblot analysis with glycogen synthase kinase-3 as a substrate. Western blots were quantified by densitometry and relative intensities of each band are shown.

in vitro assay of Akt-catalyzed phosphorylation of GSK3 (Fig. 3D). The catalytic activity of Akt was increased in wild-type DT40 cells by serum starvation. The activation of the PI3K/Akt pathway might be related to the cell survival of wild-type DT40 cells under stress conditions. Second, serum starvation induced phosphorylation of c-Jun and JNK in AIB1-deficient cells, not in wild type cells (Fig. 3B). Because both of AIB1$^{+/-}$ and AIB1$^{-/-}$ cells were killed by FCS deprivation (Fig. 2B), there are good correlation between the activation of JNK/c-Jun pathway

and the cell death. The stress-activated JNK pathway might be related to the cell death of AIB1-deficient cells under stress condition. On the other hand, there was no difference in the p38 MAPK/ERK pathway (Fig. 3C). Taken together, our data suggest that AIB1 acts as a molecular link between Akt/p65-induced cell survival and JNK/c-Jun-regulated cell death in response to cellular stress.

In Fig. 3A, a band was observed in the panel for $AIB1^{-/-}$ cells. This weak signal was found in all lanes using anti-AIB1 antibody, although it was difficult to identify because it was just above the specific band. Possibly, our AIB1-antibody might cross-react to the closely related protein such as TIF2 or SRC1.

Cellular Stress Induces Upregulation of AIB1 Gene Expression—To test directly whether cellular stress causes increased AIB1 gene expression by modulating Akt function or cell cycle regulators in GI/S transition, we examined the levels of expression of the mRNAs of various cell cycle regulators by Northern blotting in wild-type or AIB1-knockout DT40 cells after stimulation by serum starvation (Fig. 4). The mRNA levels of all the regulators investigated in AIB1-knockout cells were decreased efficiently by serum starvation. In contrast, the mRNA levels of AIB1, Akt, and RSK2 in wild-type DT40 cells were increased significantly by serum deprivation. No notable increases in mRNA levels of the G1/S-cell cycle regulators cyclin D1, cyclin D2, cyclin E and E2F1 were found in wild-type DT40 cells under serum starvation. These data indicate that, under cellular stresses such as serum starvation, high levels of AIB1 mRNA are mediated by Akt or RSK2, but not by activation of the regulators of cell cycle progression in the G1/S phase. Accordingly, cellular stress-induced AIB1 amplification may enhance cell survival and DNA replication through coordinated upregulation of the Akt signaling pathway.

AIB1 Is Essential for Induction of Akt-Dependent DNA Replication in Response to Cellular Stress—To assess the role of AIB1 in mediating Akt-activated DNA replication in response to cellular stress, we analyzed the contribution of phosphorylated Akt at designated time points after synchronization of the cell cycle by treatment with hydroxyurea, which arrests the cycle in the early S-phase. While we observed no differences in the low levels of Akt phosphorylation during synchronization, phosphorylation of Akt was blocked in AIB1-knockout DT40 cells, unlike in wild-type cells, after release of the cell cycle arrest. In contrast, induction of Akt phosphorylation was significantly increased in wild-type cells when they were released from arrest and progressed further into S phase (Fig. 5A). By treatment with the pharmacological agent LY294002, an inhibitor of PI3K/Akt kinase, we next investigated whether the requirement for AIB1 in DNA replication was dependent on Akt in stressed cells. Wild-type DT40 cells with LY294002 had marked decreased numbers of BrdU-positive cells (Fig. 5B), suggesting that, in wild-type cells, inhibition of cell cycle progression into S phase occurred by the inhibition of Akt, in the same way as in AIB1-knockout cells. Inhibition of MAPK activity by treatment with PD98059 did not lead to a marked decrease in DNA replication in response to serum starvation in wild-type DT40 cells (data not shown). Thus, these results indicate that induction of Akt phosphorylation as a consequence of progression into S phase caused a requirement for AIB1 in DNA replication in response to cellular stress.

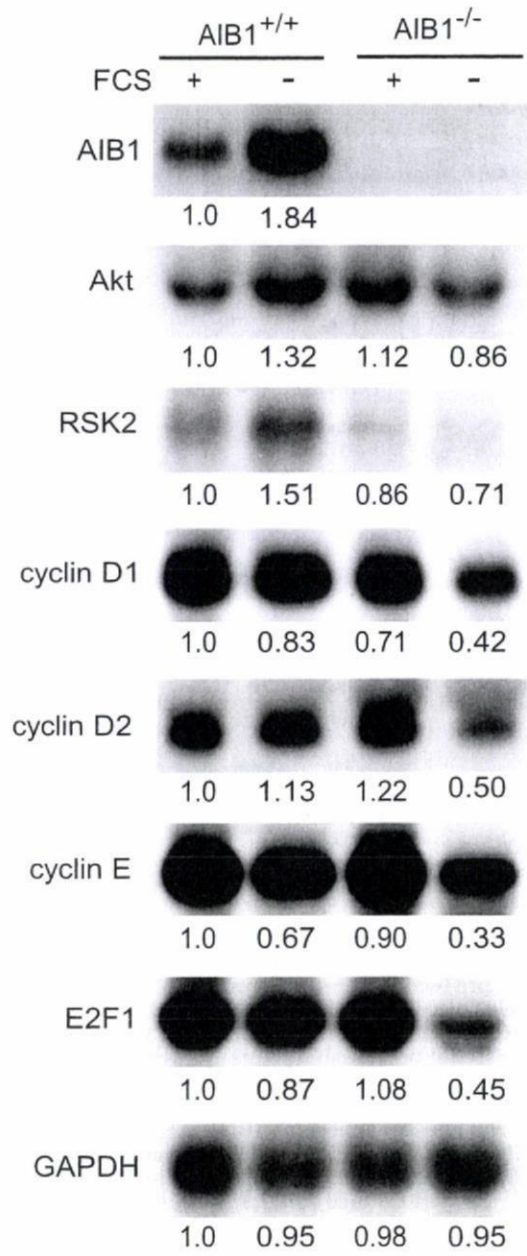

Fig. 4. **Relative levels of expression of mRNAs of cell cycle regulators.** Wild-type and AIB1-knockout DT40 cells were cultured for 8 h in the presence or absence of FCS. Total RNAs were prepared for Northern blot analysis. The radioactivities of the corresponding bands of cell cycle regulators and GAPDH mRNA were determined with an image analyzer as relative intensity, and the normalized intensity against levels of mRNA in wild-type DT40 cells with FCS are shown.

Recent study showed that AIB1 overexpression enhanced the activation of PI3K/Akt pathway and AIB1 knockdown increased apoptosis (*15*). As mentioned above, the stress-activated JNK pathway was suppressed in the presence of AIB1 (Fig. 3B). In order to investigate if the JNK suppression is mediated by the PI3K/Akt pathway, we

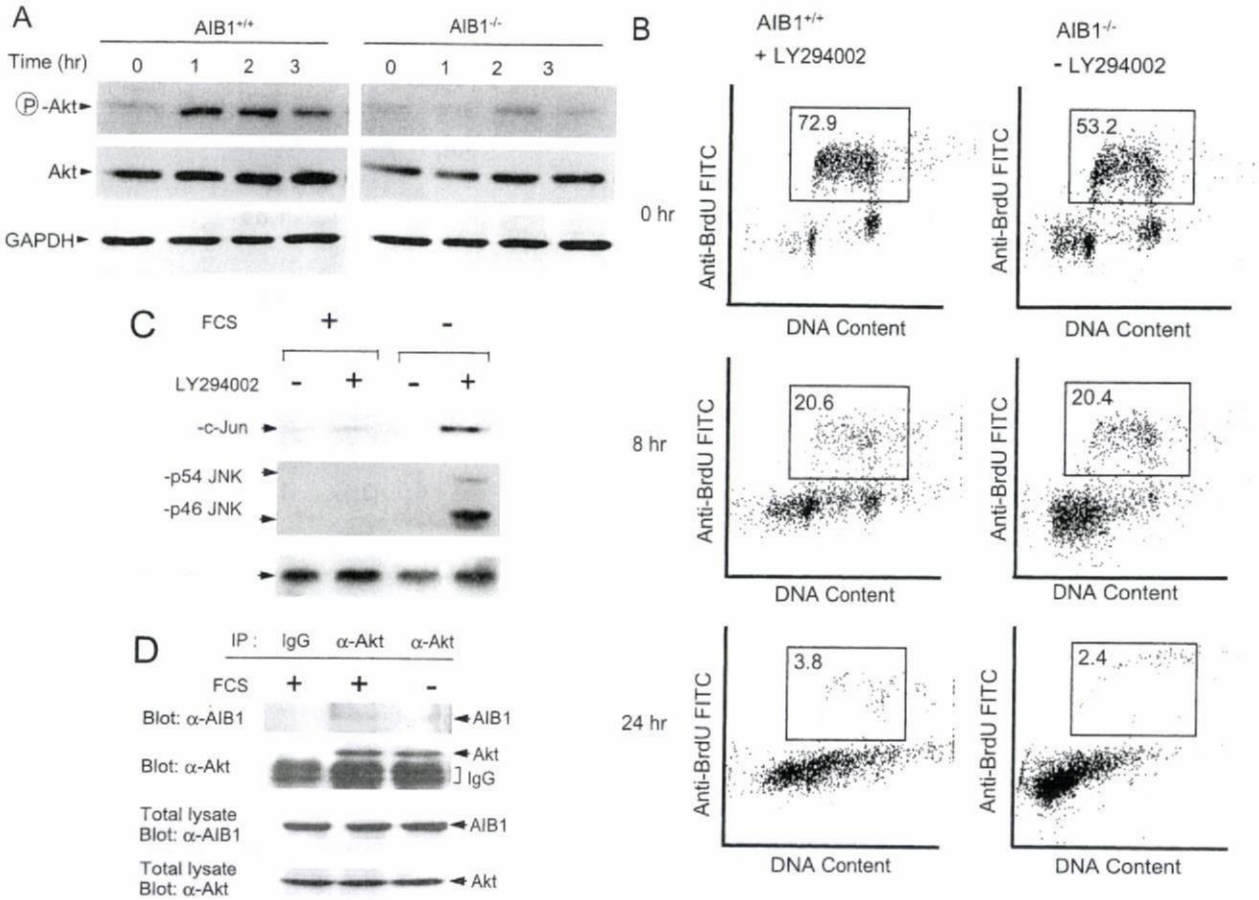

Fig. 5. **Inhibition of Akt or deficiency of AIB1 blocks DNA replication under stress conditions.** (A) Akt phosphorylation and AIB1 production were required for DNA replication. Cells were synchronized for 8 h with hydroxyurea (1 mM), which interfered with cell cycle progression by preventing DNA replication, and were harvested at the indicated points (0–3 h) following release from the cell cycle arrest. Production of phosphorylated Akt and total Akt was determined by immunoblot analysis using anti-phospho-Akt (Ser-473) and anti-Akt antibodies. (B) DNA replication in wild-type DT40 cells by in response to serum deprivation was blocked by LY294002, an inhibitor of PI3K/Akt. Wild-type cells or AIB1-knockout cells were cultured with LY294002 (50 μM) in the absence of FCS for 8 h or 24 h. The percentage BrdU positivity was determined by counting the number of cells at the BrdU-positive gates. (C) The JNK suppression in the AIB1-positive cells was blocked by LY294002. Wild-type cells were cultured with or without LY294002 (50 μM) in the presence or absence of FCS for 8 h. The levels of phosphoprotein in the JNK-mediated apoptosis pathway were determined by Western blot. (D) AIB1 is physically associated with Akt. The DT40 cell extracts were immunoprecipitated with anti-Akt antibody. For control, cell extract was precipitated with the IgG from non-immunized rabbit. The immunoprecipitates (IP) were subjected to Western blot analysis with the indicated antibodies.

examined the phosphorylation of c-Jun and JNK after LY294002 treatment. As a result, we found the marked increase of phospho-c-Jun and phospho-JNK by the LY294002 treatment in response to serum starvation (Fig. 5C), suggesting that the inhibition of PI3K/Akt pathway blocked the AIB1-mediated JNK suppression. Further, we showed the direct interaction between AIB1 and Akt (Fig. 5D). Collectively, these data suggested that AIB1 might be activated by Akt.

Loss of AIB1 Leads to Inhibition of UV-Induced Phosphorylation of Histone H3 at Serine 10—DNA replication is linked to chromatin modulation. This is associated with the modification of chromatin-associated proteins such as histones (H2A, H2B, H3, and H4) or remodeling cofactors, which are known to possess intrinsic histone acetyltransferase activity and are capable of chromatin modification by histone acetylation (*9*, *10*). We have shown here that AIB1 depletion causes a marked defect in the ability to induce DNA replication in response to cellular stress. Therefore, AIB1 may control the signal cascades for the remodeling of chromatin in response to cellular stress. We next examined whether AIB1 was required for phosphorylation of chromatin modulation in response to cellular stress. By Western blot analyses using cell extracts of acid-soluble proteins, we found that wild-type cells had a marked increase in the phosphorylation of histone H3 at serine 10 (Fig. 6), but not in the acetylation of histone H3 at lysine 9 or 14 (data not shown), very soon after treatment with UV-irradiation. This phosphorylation was completely eliminated under stress conditions by the loss of AIB1 in AIB1-knockout cells (Fig. 6). Although a previous study had shown that AIB1 possesses intrinsic histone acetyltransferase (HAT) activity for chromatin modification (*2*), we observed no difference in the levels of acetylation of histone H3 at lysine 9 and lysine 14 in AIB1-knockout DT40 cells compared with wild-type cells

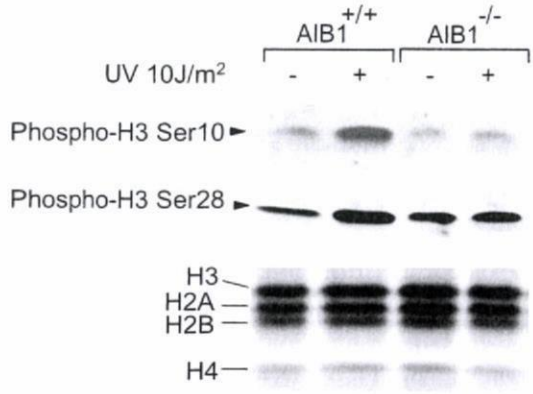

Fig. 6. **Knockout of AIB1 leads to inhibition of UV-induced phosphorylation of histone H3 at serine 10.** Western blot analyses are shown with the specific antibodies indicated on the left, in wild-type or AIB1-knockout cells either treated or untreated by UV irradiation (10 J/m^2). Coomassie Blue–stained 15% polyacrylamide SDS–containing gels indicated equal loading of proteins.

following UV irradiation (data not shown). These results suggest that AIB1 plays a critical role in the signaling cascade for both Akt activation and modulation of the phosphorylation of histone H3 at serine 10 in response to cellular stress.

DISCUSSION

Recent studies have demonstrated that AIB1 plays a pivotal role in activation of the intrinsic IGF-1–driven cell survival pathway, which is mediated through the PI3K/Akt pathway (*15*). Although the signal transduction pathways that lead to the positive control of AIB1 have been studied extensively, the critical targets of this kinase that mediate the stress response remain to be determined. We showed here that AIB1-deficient DT40 cells are extremely sensitive to be killed by cellular stresses such as serum deprivation and UV irradiation. This susceptibility was correlated with a reduction in the ability to restore DNA-synthesis levels under stress conditions. Moreover, we showed that, with serum deprivation or UV irradiation treatment, the induction of phosphorylation of both JNK and c-Jun in AIB1-knockout DT40 cells was much greater than in wild-type DT40 cells. These results are consistent with those of previous studies, which demonstrated that activation of the JNK/c-Jun pathway mediates the induction of cell death by DNA damage agents (*33, 34*). Our results therefore indicate that the presence of AIB1 is required to suppress activation of the JNK/c-Jun signaling pathway in DNA replication under cellular stress conditions. On the other hand, in ER-negative cancer cells subjected to cellular stress, high levels of AIB1 production have been shown to promote activation of the Akt/p65 survival pathway (*15*). It has been shown that activation of c-Jun by the JNK apoptosis pathway is required to suppress NF-κB transcription (*35, 36*). Our study is consistent with the result of a recent report, which demonstrated that Akt inhibits stress-activated JNK through activation of NF-κB (*36*). Collectively, these data indicate that AIB1 plays a key role as a mediator between the Akt/NF-κB and JNK/c-Jun pathways in controlling cell fate in response to cellular stress.

Importantly, various signal transduction pathways can modulate the interactions of specific coregulators with nuclear receptors or mediate their activities (*37*). Recent studies suggest that the transcriptional corepressors NCoR and SMRT interact with, and exert repressive effects on AP-1 or NF-κB (*38–41*). It has been proposed that the transactivation potential of c-Jun is repressed by histone deacetylase (HDAC) complexes and these repressor complexes are dissociated by JNK-mediated phosphorylation (*42*). As can be seen from our stress assays in DT40 cells, presence of AIB1 is an important key to modulate the switch from transcriptional repression to activation in association with the diverse protein kinase-dependent signalling pathways in response to cellular stress.

We have shown that, in addition to its role in signal ransduction pathways, AIB1 production is correlated with UV-induced phosphorylation of histone H3 at serine 10, but not with acetylation of histone H3 at lysine 9 or 14. These results suggest that AIB1 is essential in mediation of the phosphorylation of histone H3 in chromatin remodeling. Although it has been shown that the phosphorylation of histone H3 is mediated by the Aurora B kinases (*43*), IKK-α (*45*), MSK1 and MSK2 (*45*), and RSK-2 (*46*), we need to reveal by future studies a kinase that can phosphorylate histone H3 in association with AIB1 directly. Previous studies have reported that IκB kinase, a positive regulator of NF-κB activation, is activated by Akt (*13, 14*). However, production of endogenous IKKα or IKKβ proteins did not change detectably in response to activated Akt in DT40 cells (data not shown). NF-κB activation by stress stimuli has also been shown to be independent of phosphorylation of IκBα at Ser 32/36, and to be IKK-independent (*47*). Moreover, NF-κB, which is usually maintained in an inactive state by protein–protein interaction with inhibitor IκBs, is constitutively active in ER-negative breast cancer cell lines (*48*). Thus, in DT40 cells AIB1 might be produced as one of the downstream targets interacting directly with Akt, independently of IKK.

Previous studies have found that, under conditions of stress, Akt interacts with JIP1 in primary neurons and thus inhibits JNK activation. Therefore, ectopic expression of Akt attenuated stress-induced apoptosis while Akt1 gene deletion rendered neurons more sensitive to stress stimulus than wild-type neurons (*49*). Moreover, recent studies have shown that activation of NF-κB is required for inhibition of JNK in response to TNF-α or UV stimulation (*21–24*). These previous studies and our findings suggest that the level of production of AIB1 is a key determinant of cell susceptibility to cellular stress, in association with phosphorylation cascades. Furthermore, we have elucidated the molecular mechanisms by which, in response to cellular stress, AIB1 plays a critical role in DNA replication or phosphorylation of histone H3 at serine 10, in association with active Akt/NF-κB pathway.

We thank Shunichi Takeda and Shigehiro Osada for their helpful discussions, and Madaka Tsuruta for expert assistance with the cell culture. This work was supported in part by grant from Health and Labor Science Research Grants from the Ministry of Health, Labor and Welfare of Japan.

REFERENCES

1. Anzick, S.L., Kononen, J., Walker, R.L., Azorsa, D.O., Tanner, M.M., Guan, X.Y., Sauter, G., Kallioniemi, O.P., Trent, J.M., and Meltzer, P.S. (1997) AIB1, a steroid receptor coactivator amplified in breast and ovarian cancer. *Science* **277**, 965–968
2. Chen, H., Lin, R.J., Schiltz, R.L., Chakravarti, D., Nash, A., Nagy, L., Privalsky, M.L., Nakatani, Y., and Evans, R.M. (1997) Nuclear receptor coactivator ACTR is a novel histone acetyltransferase and forms a multimeric activation complex with P/CAF and CBP/p300. *Cell* **90**, 569–580
3. Torchia, J., Rose, D.W., Inostroza, J., Kamei, Y., Westin, S., Glass, C.K., and Rosenfeld, M.G. (1997) The transcriptional co-activator p/CIP binds CBP and mediates nuclear-receptor function. *Nature* **387**, 677–684
4. Takeshita, A., Cardona, G.R., Koibuchi, N., Suen, C.S., and Chin, W.W. (1997) TRAM-1, a novel 160-kDa thyroid hormone receptor activator molecule, exhibits distinct properties from steroid receptor coactivator 1. *J. Biol. Chem.* **272**, 27629–27634
5. Li, H., Gomes, P.J., and Chen, J.D. (1997) RAC3, a steroid/nuclear receptor associated coactivator that is related to SRC-1 and TIF2. *Proc. Natl. Acad. Sci. USA* **94**, 8479–8484
6. Onate, S.A., Tsai, S.Y., Tsai, M.J., and O'Malley, B.W. (1995) Sequence and characterization of a coactivator for the steroid hormone receptor supperfamily. *Science* **270**, 1354–1357
7. Voegel, J.J., Heine, M.J., Zechel, C., Chambon, P., and Gronemeyer H. (1996) TIF2, a 160 kDa transcriptional coactivator for the ligand-dependent activation function AF-2 of nuclear receptors. *EMBO J.* **15**, 3667–3675
8. Hong, H., Kohli, K., Garabedian, M.J., and Stallcup, M.R. (1997) . GRIP1, a transcriptional coactivator for the AF-2 transactivation domain of steroid, thyroid, retinoid, and vitamin D receptors. *Mol. Cell Biol.* **17**, 2735–2744
9. Huang, Z.Q., Li, J., Sachs, L.M., Cole, P.A., and Wong, J. (2003) A role for cofactor-cofactor and cofactor-histone interactions in targeting p300, SWI/SNF and Mediator for transcription *EMBO J.* **22**, 2146–2155
10. Dilworth, F.J., Fromental-Ramain, C., Yamamoto, K., and Chambon, P. (2000) ATP-driven chromatin remodeling activity and histone acetyltransferases act sequentially during transactivation by RAR/RXR In vitro. *Mol. Cell* **6**, 1049–1058
11. Osborne, C.K., Bardou, V., Hopp, T.A., Chamness, G.C., Hilsenbeck, S.G., Fuqua, S.A., Wong, J., Allred, D.C., Clark, G.M., and Schiff R. (2003) Overexpression of the steroid receptor coactivator AIB1 in breast cancer correlates with the absence of estrogen and progesterone receptors and positivity for p53 and HER2/neu. *J. Nat. Cancer Inst.* **95**, 353–361
12. Bouras, T., Southey, M.C., and Venter, D.J. (2001) Overexpression of the steroid receptor coactivator AIB1 in breast cancer correlates with the absence of estrogen and progesterone receptors and positivity for p53 and HER2/neu. *Cancer Res.* **61**, 903–907
13. Ozes. O.N., Mayo, J.A., Gustin, S.R., Pfeffer, L.M., and Donner, D.B. (1999) NF-κB activation by tumour necrosis factor requires the Akt serine-threonine kinase. *Nature* **401**, 82–85
14. Romashkova, J.A. and Makarov, S.S. (1999) NF-κB is a target of AKT in anti-apoptotic PDGF signalling. *Nature* **401**, 86–90
15. Torres-Arzayus, M.I., De Mora, J.F., Yuan, J., Vazquez, F., Bronson, R., Rue. M., Sellers, W.R., and Brown, M. (2004) High tumor incidence and activation of the PI3K/AKT pathway in transgenic mice define AIB1 as an oncogene. *Cancer Cell* **6**, 263–274
16. Werbajh S, Nojek I, Lanz R., and Costas, M.A. (2000) RAC-3 is a NF-κB coactivator. *FEBS Lett.* **485**, 195–199
17. Wu, R.C., Qin, J., Hashimoto, Y., Wong, J., Xu, J., Tsai, S.Y., Tsai, M.J., and O'Malley, B.W. (2002) Regulation of SRC-3 (pCIP/ACTR/AIB-1/RAC-3/TRAM-1) Coactivator activity by I kappa B kinase. *Mol. Cell Biol.* **22**, 3549–3561
18. Nakshatri, H., Bhat-Nakshatri, P., Martin, D.A., Goulet, JR, R.J., and Sledge, JR., G.W. (1997) Constitutive activation of NF-κB during progression of breast cancer to hormone-independent growth. *Mol. Cell Biol.* **17**, 3629–3639
19. Sheppard, K.A., Rose, D.W., Haque, Z.K., Kurokawa, R., McInerney, E., Westin, S., Thanos, D., Rosenfeld, M.G., Glass, C.K., and Collins, T. (1999) Transcriptional activation by NF-κB requires multiple coactivators. *Mol. Cell Biol.* **19**, 6367–6378
20. Davis, R.J. (2000) Signal transduction by the JNK group of MAP kinases. *Cell* **103**, 239–252
21. Liu, J. and Lin, A. (2005) Role of JNK activation in apoptosis: a double-edged sword. *Cell Res.* **15**, 36–42
22. Tang, G., Minemoto, Y. Dibling, B., Purcell, N.H. Li, Z., Karin, M., and Lin, A. (2001) Inhibition of JNK activation through NF-kappaB target genes. *Nature* **414**, 313–317
23. Tang, F., Tang, G., Xiang, J., Dai, Q., Rosner, M.R., and Lin, A. (2002) The absence of NF-kappaB-mediated inhibition of c-Jun N-terminal kinase activation contributes to tumor necrosis factor alpha-induced apoptosis. *Mol. Cell Biol.* **22**, 8571–8579
24. Lin, A. (2003) Activation of the JNK signaling pathway: breaking the brake on apoptosis. *Bioessays* **25**, 17–24
25. Verger, A. and Crossley, M. (2004) Chromatin modifiers in transcription and DNA repair. *Cell. Mol. Life Sci.* **61**, 2154–2162
26. Nowak, S.J. and Corces, V.G. (2004) Phosphorylation of histone H3: a balancing act between chromosome condensation and transcriptional activation. *Trends Genet.* **20**, 214–220
27. Hueber, A.O. and Evan, G. (1998) Traps to catch unwary oncogenes. *Trends Genet.* **14**, 364–367
28. Baba, T.W., Giroir, B.P., and Humphries, E.H. (1985) Cell lines derived from avian lymphomas exhibit two distinct phenotypes. *Virology* **144**, 139–151
29. Arai, S., Ogawa, K., Yamachika, S., Nishihara, T., and Nishikawa, J. (2001) Cloning and functional characterization of chicken p160 coactivator family members. *Biochim. Biophys. Acta* **1518**, 7–18
30. Karin, M. (1998) Mitogen-activated protein kinase cascades as regulators of stress responses. *Ann. N.Y. Acad. Sci.* **851**, 139–146
31. Tournier, C., Hess, P., Yang, D.D., Xu, J., Turner, T.K., Nimual, A., Bar-Sagi, D., Jones, S.N., Flavell, R.A., Davis, R.J. (2000) Requirement of JNK for stress-induced activation of the cytochrome c-mediated death pathway. *Science* **288**, 870–874
32. Chang, L. and Karin, M. (2001) Mammalian MAP kinase signalling cascades. *Nature* **410**, 37–40
33. Chen, Y.R., Wang, X., Templeton, D., Davis, R.J., and Tan, T.H. (1996) The role of c-Jun N-terminal kinase (JNK) in apoptosis induced by ultraviolet C and gamma radiation. Duration of JNK activation may determine cell death and proliferation. *J. Biol. Chem.* **271**, 31929–31936
34. Faris, M., Kokot, N., Latiinis, K., Kasibhatla, S., Green, D.R., Koretzky, G.A., and Nel, A. (1998) The c-Jun N-terminal kinase cascade plays a role in stress-induced apoptosis in Jurkat cells by up-regulating Fas ligand expression. *J. Immunol.* **160**, 134–144
35. Reuther-Madrid, J.Y., Kashatus, D., Chen, S., Li, X., Westwick, J., Davis, R.J., Earp, H.S., Wang, C-Y., and Baldwin Jr., A.S. (2002) The p65/RelA subunit of NF-kappaB suppresses the sustained, antiapoptotic activity of Jun kinase induced by tumor necrosis factor. *Mol. Cell Biol.* **22**, 8175–8183
36. Yuan, Z., Feldman, R.I., Sun, M., Olashaw, N.E. Coppola, D., Sussman, G.E., Shelley, S.A., Nicosia, S.V., and Cheng, Q. (2002) Inhibition of JNK by cellular stress- and tumor necrosis factor alpha-induced AKT2 through activation of the NF kappa B pathway in human epithelial Cells. *J. Biol. Chem.* **277**, 29973–29982

37. Rosenfeld, M.G. and Glass, C.K. (2001) Coregulator codes of transcriptional regulation by nuclear receptors. *J. Biol. Chem.* **276**, 36865–36868
38. Zhang, J., Kalkum, M., Chait, B.T., and Roeder, R.G. (2002) The N-CoR-HDAC3 nuclear receptor corepressor complex inhibits the JNK pathway through the integral subunit GPS2. *Mol. Cell* **9**, 611–623
39. Perissi, V., Aggarwal, A., Glass, C.K., Rase, D.W., and Rosenfeld, M.G. (2004) A corepressor/coactivator exchange complex required for transcriptional activation by nuclear receptors and other regulated transcription factors. *Cell* **116**, 511–526
40. Lee, S.K., Kim, J.H., Lee, Y.C., Cheong, J. and Lee, J.W. (2000) Silencing mediator of retinoic acid and thyroid hormone receptors, as a novel transcriptional corepressor molecule of activating protein-1, nuclear factor-kappaB, and serum response factor. *J. Biol. Chem.* **275**, 12470–12474
41. Baek, S.H., Ohgi, K.A., Rose, D.W., Koo, E.H., Glass, C.K., and Rosenfeld, M.G. (2002) Exchange of N-CoR corepressor and Tip60 coactivator complexes links gene expression by NF-kappaB and beta-amyloid precursor protein. *Cell* **110**, 55–67
42. Weiss, C., Schneider, S., Wagner, E.F., Zhang, X., Seto, E., and Bohmann, D. (2003) JNK phosphorylation relieves HDAC3-dependent suppression of the transcriptional activity of c-Jun. *EMBO J.* **22**, 3686–3695
43. Clayton, A.L. and Mahadevan, L.C. (2003) MAP kinase-mediated phosphoacetylation of histone H3 and inducible gene regulation. *FEBS Lett.* **546**, 51–58
44. Yamamoto, Y., Verma, U.N., Prajapati, S., Kwak, Y.T., and Gaynor, R.B. (2003) Histone H3 phosphorylation by IKK-alpha is critical for cytokine-induced gene expression. *Nature* **423**, 655–659
45. Soloaga, A., Thomson, S., Wiggin, G.R., Rampersaud, N., Dyson, M.H., Hazzalin, C.A., Mahadevan, L.C., and Arthur, J.S. (2003) MSK2 and MSK1 mediate the mitogen- and stress-induced phosphorylation of histone H3 and HMG-14. *EMBO J.* **22**, 2788–2797
46. Sassone-Corsi, P., Mizzen, C.A., Cheung, P., Crosio, C., Monaco, L., Jacquot, S., Hanauer, A., and Allis, C.D. (1999) Requirement of Rsk-2 for epidermal growth factor-activated phosphorylation of histone H3. *Science* **285**, 886–891
47. Li, N. and Karin, M. (1998) Ionizing radiation and short wavelength UV activate NF-kappaB through two distinct mechanisms. *Proc. Natl. Acad. Sci. USA* **95**, 13012–13017
48. Tergaonkar, V., Bottero, V., Ikawa, M., Li, Q., and Verma, I.M. (2003) IkappaB kinase-independent IkappaBalpha degradation pathway: functional NF-kappaB activity and implications for cancer therapy. *Mol. Cell Biol.* **23**, 8070–8083
49. Kim, A.H., Yano, H., Cho, H., Meyer, D., Monks, B., Margolis, B., Birnbaum, M.J., and Chao, M. V. (2002) Akt1 regulates a JNK scaffold during excitotoxic apoptosis. *Neuron* **35**, 697–709

Anti-Androgenic Activity of *N*-Nitrosodibenzylamine, *N*-Nitrosodiphenylamine and *N*-Nitrosodicyclohexylamine

Sayaka Hari,[a] Jun-ichi Nishikawa,[a] Kikumi Horiguchi,[a] Mitsuru Iida,[b] and Tsutomu Nishihara*[,a,1]

[a]*Laboratory of Environmental Biochemistry, Graduate School of Pharmaceutical Sciences, Osaka University, 1–6 Yamada-oka, Suita, Osaka 565–0871, Japan and* [b]*EDC Analysis Center, Otsuka Pharmaceutical Company LTD., Kawauchi, Tokushima 771–0132, Japan*

(Received February 16, 2006; Accepted June 12, 2006; Published online July 3, 2006)

When 56 selected environmental chemicals were tested for the androgenic activity to Yeast Two-hybrid and reporter gene assay in the presence of 5α-dihydrotestosterone (DHT), the activity was inhibited by some of the chemicals including *N*-nitrosodiphenylamine (NDPA), a novel anti-androgenic compound, and one of suspected carcinogenic *N*-nitrosocompounds (NOCs) commonly used as material of rubber and plastic goods. We further examined 15 NOCs for anti-androgenic activity, and found that *N*-nitrosodibenzylamine (NDBzA) and *N*-nitrosodicyclohexylamine (NDCHA) as well as NDPA inhibited the activity of DHT in a dose-dependent manner. These compounds showed the competitive binding to androgen receptor (AR) against DHT and decreased the level of AR protein. Furthermore, 3 NOCs down-regulated the prostate specific antigen (PSA) at the transcriptional level in LNCaP cells. These results suggest that some NOCs antagonized the androgenic effect of DHT in the same manner as the synthetic anti-androgen, flutamide (F).

Key words —— anti-androgenic activity, androgen receptor, *N*-nitrosocompound, *N*-nitrosodibenzylamine, *N*-nitrosodiphenylamine, *N*-nitrosodicyclohexylamine

INTRODUCTION

The androgens, testosterone (T) and its metabolite 5α-dihydrotestosterone (DHT), play an important role in the development and function of male reproductive organs such as prostate and testis, as well as non-reproductive organs including muscle, hair follicles and brain. Their biological effects are mediated by one of the nuclear receptor superfamily of ligand-regulated transcription factors, androgen receptor (AR).[1,2] T is synthesized mainly in the Leydig cells of testes and converted in the prostate to DHT, a more potent androgen than T. Upon DHT binding to AR in the cytosol, the complex translocates to the nucleus, where AR-DHT complex binds to androgen response element (ARE) in the promoter region of target genes and regulate the transcription of them.[3,4] The androgen target gene, a member of the human kallikrein gene family, produces prostate specific antigen (PSA), which is well known as a marker protein of prostate cancer.[5]

It has been noticed that some environmental and industrial chemicals interfere with endogenous androgen function in humans and wildlife. These compounds are referred to as endocrine disruptors (EDs). Interference with androgenic action can occur in a various developmental and reproductive abnormalities of the male sex functions.[6] Although there have been many reports on EDs, most of them are estrogenic action via estrogen receptor (ER). We therefore have been focused on anti-androgenic compounds, showing female phenotype via AR.

There have been many studies of screening for EDs by *in vitro* assays, such as Yeast Two-hybrid, reporter gene, and receptor binding assay.[7–10] Environmental anti-androgens, such as *p,p'*-dichlorodiphenyldichloroethylene (DDE), vinclozolin and linuron, compete with endogenous androgens for AR, to alter androgen-dependent transcriptions by inhibition of binding to AR.[11–16] Now more than

[1]Present address: Osaka University, Center for Advanced Science and Innovation, A-407, 2–1 Yamada-oka, Suita, Osaka 565–0871, Japan.

*To whom correspondence should be addressed: Osaka University, Center for Advanced Science and Innovation, A-407, 2–1 Yamada-oka, Suita, Osaka 565–0871, Japan. Tel.: +81-6-6879-7423; Fax: +81-6-6879-7426; E-mail: r-nishihara@dol.hi-ho.ne.jp

50000 chemicals are distributed in the world, among which novel and potent anti-androgenic chemicals may exist. We should therefore assess androgenic action of these chemicals before they affect to humans and wildlife.

In this study, we first tested anti-androgenic activity of a total of 56 environmental chemicals by Yeast Two-hybrid and AR-EcoScreen cell reporter gene assay. These were performed flutamide (F) and hydroxyflutamide (HF) as a positive compound. F is well known as a synthetic anti-androgen and used for drug therapy of prostate cancer.[17] HF is an active metabolite of F.

We found a novel anti-androgenic compound, *N*-nitrosodiphenylamine (NDPA). *N*-Nitroso compounds (NOCs) including NDPA are well known to have carcinogenic and mutagenic properties, such that gastric, esophageal, nasopharyngeal, bladder and colon cancers.[18,19] However there have been no reports that NOCs affect endocrine systems. Exposure to environmental NOCs is through various pathways, for example, life-style (tobacco, food, cosmetic products and household commodities), occupational (rubber, leather, and material industry) and uptake of precursors (nitrite, nitrate and amine).[20] Thus it is thought that humans and wildlife have chance affected by NOCs. Then we tested anti-androgenic activity of 15 NOCs by using Yeast Two-hybrid and reporter gene assay. Finally we investigated the mechanism of anti-androgenic action of positive compounds.

MATERIALS AND METHODS

Chemicals and Cells —— All chemicals of the highest grade commercially available were used without further purification. Most of 56 test chemicals listed in Table 1 are the same used in the previous paper.[7] NOCs listed in Table 2 were purchased from Wako Pure chemicals (Osaka, Japan) and dissolved in dimethyl sulfoxide (DMSO) for use. AR EcoScreen cells were grown in 10 cm dishes using DMEM/F-12 (GIBCO, BRL, Inc., U.K.) supplemented with 5% heat-inactivated fetal bovine serum (FBS, ICN Biomedical, Inc., Aurora, Ohio), penicillin (100 U/ml), streptomycin (100 μg/ml) (Nakarai Tesque Co., Kyoto, Japan) in a humidified 5% CO_2 incubator. LNCaP cells, the androgen-sensitive human prostate cancer cell line, were cultured in 10 cm dishes using RPMI 1640 (Nacalai Tesque Co., Kyoto, Japan) supplemented with 10% FBS, penicillin (100 U/ml) and streptomycin (100 μg/ml) (Nacalai Tesque Co., Kyoto, Japan) in a humidified 5% CO_2 incubator.

Yeast Two-Hybrid Assay (AR:SRC-1) —— The Yeast Two-hybrid assay system with the rat AR and the coactivator, steroid receptor coactivator-1 (SRC-1), was prepared by modifying the method described in previous reports.[7,21] Briefly, two expression plasmids, pGBT9-AR-LBD and pACT2-SRC-1, were transformed into yeast cells (Saccharomyces cerevisiae Y190). The yeast cells (100 μl), pre-incubated overnight at 30°C in synthetic defined (SD) medium free from tryptophan and leucine, were incubated with NOCs (2.5 μl) and DHT (40 nM final concentration) in SD medium lacking tryptophan and leucine (150 μl) at 30°C for 4 hr. After the absorbance at 595 nm was measured, the cultured cells were digested enzymatically with zymolyase 20T (Seikagaku Co., Tokyo, Japan) at 37°C for 15 min. Then the lysate was mixed with 40 μl of *o*-nitrophenyl-β-D-galactopyranoside (4 mg/ml in Z-buffer) and incubated at 37°C for 1 hr. Finally, added 100 μl of 1 M Na_2CO_3 to stop the reaction and then absorbance at 420 and 570 nm were measured by using a 96-well microplate reader (Model 550 MICROPLATE READER, BIO RAD) and β-galactosidase activity was calculated from these 3 absorbances. The anti-androgenic activity was expressed as the percentage against β-galactosidase activity of 40 nM DHT without chemicals (100%). It was judged to be positive when the inhibition was more than 20% and the cytotoxicity was not observed at these concentrations. Cytotoxicity of the compound was confirmed by using control yeast cells which transformed pGBT9-p53 and pGAD3F-SV40 into yeast cells. IC_{50} values were calculated using GraphPad Prism 2.01 software.

Reporter Gene Assay for AR (AR-EcoScreen) —— The reporter gene assay using AR-EcoScreen cells was performed as previously described.[22] AR EcoScreen can evaluate androgenic activity and toxicity of compound. Briefly, in 24 well plates, AR-EcoScreen cells were seeded 1×10^5 cells/ml in phenol red free DMEM/F12 containing 5% charcoal-dextran treated fetal bovine serum (FBS). After 24 hr of culturing, medium was changed and added NOCs with 0.5 nM DHT. Following 16–24 hr of culturing, cells were washed twice with phosphate buffered saline (PBS), lysed with Passive Lysis Buffer (Promega Co., WI, U.S.A.) and assayed using Dual luciferase assay system (Promega Co., WI, U.S.A.) with luminometer (Lumat LB9501, Berthold

Table 1. Names of 56 Test Chemicals and Anti-Androgenic Activity in the Yeast Two-Hybrid Assay (AR:SRC-1)

Group, compounds[a]	
Pesticides and related (21)	Benzens and heterocyclics (9)
1,2-Dibromo-3-chloropropane	2,4-Dinitroaniline
2,4,5-Trichlorophenol	2,5-Dinitroaniline
2,4-Dichlorophenoxyacetic acid	2-Phenylendiamine
2,4,5-Trichlorophenoxyacetic acid	4-Chloroaniline
Alachlor[b]	Benzophenone[b]
Aldicarb	Biphenyl[b]
Captan	*N*-Ethylaniline
Carbaryl (NAC)[b]	4-Nitrotoluene
γ-Hexachlorocyclohexane (γ-HCH)[b]	*N*-Nitrosodiphenylamine (NDPA)[b]
Hexachlorophene[b]	Phthalates and adipate (9)
Maneb	Di-*n*-ethyl phthalate[b]
Manzeb	Di-*n*-propyl phthalate[b]
Methomyl	Di-*n*-butyl phthalate[b]
Methoxychlor (MXC)	Di-*n*-pentyl phthalate
Molinate[b]	Di-*n*-hexyl phthalate
Pentachlorophenol	Butylbenzyl phthalate[b]
Thiobencarb[b]	2-Ethylhexyl phthalate
Thiuram	2-Cyclohexyl phthalate
Vinclozolin[b]	2-Ethylhexyl adipate
Simazine	Aliphatics (4)
Ziram	Cyclohexyl amine
Phenols (9)	*N*,*N*-Dimethylformamide
2,4-Dichlorophenol	Nitrilotriacetic acid
2,4-Dinitrophenol	*N*-Nitrosodimethylamine
2,4,6-Tribromophenol	Flavonoids (4)
2,5-Dichlorophenol	Coumestrol
4-Cresol	Daizein
4-Nonylphenol[b]	Genistein
Bisphenol A[b]	Naringenin
Diethylstilbesterol (DES)	
N-Phenyl-1-naphthylamine[b]	

a) Compounds marked by *b*) were positive in Yeast Two-hybrid assay (AR:SRC-1).

GmbH & Co.). The anti-androgenic activity was expressed as the percentage against 0.5 nM DHT without chemicals (100%). We judged as anti-androgen when 20% or more inhibition was calculated without cytotoxicities. IC_{50} values were calculated using GraphPad Prism 2.01 software.

Competitive Binding Assay for AR —— The binding affinity of NOCs to AR was determined by a fluorescene polarization assay using ANDROGEN RECEPTOR COMPETITOR, GREEN Kit (Pan Vera, Madison, U.S.A.). Briefly, 1 μl of NOC/DMSO solution was added to 49 μl of AL green assay buffer in the small test tube. Additionally, added 50 μl of AR-ligand binding domain (LBD) (25 nM) / Fluormone AL green (1 nM) complex to the same tube and mixed. The assay tube covered to protect the reagents from light was incubated at 22°C for 5 hr. Finally, sample fluorescence was measured on BEACON 2000 (Pan Vera, Madison, U.S.A.). DMSO (0% inhibition) instead of the compound solution was used as a negative control, and 0.5 μl of Fluormone AL green (1 nM) instead of AR-LBD/Fluormone AL green complex as a positive control (100% inhibition). IC_{50} values were calculated using GraphPad Prism 2.01 software.

Protein Preparation and Western Blotting —— LNCaP cells were seeded at 2.0×10^5 cells/ml in RPMI 1640 medium supplemented with 10% char-

Table 2. Anti-Androgenic Activity of 17 Environmental Chemicals by Yeast Two-Hybrid Assay and Reporter Gene Assay

Group, compounds	Yeast Two-hybrid assay IC_{20}[a)]	Reporter gene assay IC_{20}[b)]
Pesticides and related		
Alachlor	+	++
Carbaryl	++	−
Hexachlorophene	++	−
γ-Hexachlorocyclohexane	+	−
Molinate	+	−
Thiobencarb	++	++
Vinclozolin	++	+++
Phenols		
4-Nonylphenol	+++	++
Bisphenol A	+	++
N-Phenyl-1-naphtylamine	+	−
Benzens and heterocyclics		
Benzophenone	+	−
Biphenyl	++	−
N-Nitrosodiphenylamine (NDPA)	++	++
Phthalates		
Di-*n*-ethyl phthalate	+	−
Di-*n*-propyl phthalate	++	+++
Di-*n*- butyl phthalate	++	++
Butylbenzyl phthalate	+	+++

a) Concentration of the test compounds showing 20% inhibition of the androgenic activity induced by 40 nM DHT. *b*) Concentration of the test compounds showing 20% inhibition of the androgenic activity induced by 0.5 nM DHT. Symbols: +++, anti-androgenic activity ($IC_{20} < 1$ μM); ++, anti-androgenic activity (1 μM $\leq IC_{20} <$ 10 μM); +, anti-androgenic activity (10 μM $\leq IC_{20}$); −, no effect.

coal-stripped FBS. After 24 hr of incubating, the cells in fresh medium were incubated for 10 hr with NOCs in the presence of 10 nM DHT. After the treatment, the cells were collected Passive Lysis Buffer (Promega Co., WI, U.S.A.) and centrifuged for 5 min. The supernatant was collected as a sample of Western blotting. 15 μg aliquots were separated by SDS-PAGE (7.5% acrylamide gel) and transferred to poly(vinylidene fluoride) (PVDF) membrane. The membrane was probed with rabbit anti-androgen receptor antibody (Upstate Biotechnology, Lake Placid, NY, U.S.A.), followed by peroxidase-conjugated anti-rabbit IgG antibody (Amersham Biosciences, Piscataway, NJ, U.S.A.). The membrane was then visualized using an electrochemical luminescence (ECL) detection system.

RNA Preparation and Northern Blotting —— LNCaP cells were seeded at 1.5×10^5 cells/ml in RPMI 1640 medium supplemented with 10% charcoal-stripped FBS. After 24 hr incubation, the medium was changed and NOC was added with 10 nM DHT. After 18 hr treated, total RNA was isolated using TRIzol reagent (Invitrogen Corp., Carlsbad, CA, U.S.A.). Total RNA (12 μg) was denatured in 50% formamide and 17.5% formaldehyde at 65°C and fractionated by electrophoresis on a 1% agarose gel containing 18% formaldehyde. Samples were transferred to nylon membrane (Hybond N^+, Amersham Life Sciences, Little Chalfont, Buckinghamshire, U.K.) in 20 × SSC (1 × SSC is 0.15 M NaCl and 0.0015 M sodium citrate). The DNA probes for PSA and glyceraldehyde-3-phosphate dehydrogenase (GAPDH) were generated from PCR products. PCR primers used for PSA (418-939 bp) were: forward; 5′-GGCAGGTGCTTGTAGCCTCTC-3′, reverse; 5′-CACCCGAGCAGGTGCTTTTGC-3′, and for GAPDH: forward; 5′-ACCACAGTCCATGCCATCA-3′, reverse; 5′-TCCACCACCCTGTTGCTGTA-3′. These products were labeled with [α-^{32}P]dCTP using the BcaBEST™ Labeling Kit (TaKaRa Bio. Inc., Ohtsu, Japan). Hybridization was performed overnight at 65°C in 7% sodium dodecyl sulfate (SDS), 1% bovine serum albumin (BSA), 137 mM Na_2HPO_4

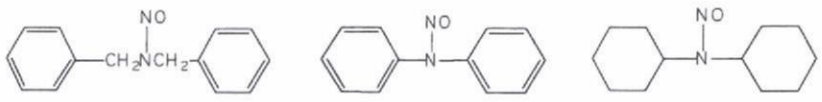

NDBzA NDPA NDCHA

Fig. 1. Chemical Structures of 3 NOCs Showing Anti-Androgenic Activity

and 63.2 mM NaH_2PO_4.

Scanning Bio-Imaging Analysis —— Scanning bio-imaging analysis was performed with a BAS-2500 (FUJI PHTO FILM Co. LTD., Kanagawa, Japan). The area of PSA was integrated by GAPDH.

Statistics —— All results are expressed as means ± standard deviations (S.D.). Statistical analysis was performed by Dunnett's method.

RESULTS

Screening for Anti-Androgenic activity of the 56 Environmental Chemicals by Yeast Two-Hybrid Assay (AR:SRC-1) and AR-EcoScreen Cell Reporter Gene Assay

For anti-androgenic activity, the test chemicals were examined in the presence of 40 and 0.5 nM DHT in Yeast Two-hybrid assay (AR:SRC-1) and AR-EcoScreen cell assay, respectively. The 2 concentrations of DHT in the assay were corresponding to 50% and 70% of the maximum activity in each assay, and it was judged to be positive for the chemicals having IC_{20} values of lower than 10 μm. Names of the 56 chemicals tested are listed in Table 1, and positive in the Yeast Two-hybrid assay were marked by *.

As seen in Table 1, about one third, 17 of the 56 chemicals, were positive in the Yeast Two-hybrid assay. When these positive compounds were applied to the cell assay, 9 of them were positive in the reporter gene assay (Table 2). The result shows that 6 (thiobencarb, vinclozolin, 4-nonylphenol, NDPA, di-n-proyl phthalate, and di-n-butyl phthalate) were agreed in both assays, but the remaining were disagreed. Except for NDPA and di-n-proyl phthalate, their anti-androgenic activities had already been reported.

Screening for Anti-Androgenic Activity on 15 NOCs

In the last section, we found that NDPA and di-n-propyl phthalate were only newly found anti-androgenic compounds. Because anti-androgenic activities of the other phthalates had been tested, we focused on the anti-androgenic activity of NDPA, and NOC with testing 15 chemicals by two *in vitro* assays. Although no androgenic activity was observed on the 15 NOCs (data not shown), 3 NOCs [*N*-nitrosodibenzylamine (NDBzA), NDPA and *N*-nitrosodicyclohexylamine (NDCHA)] shown in Fig. 1 indicated significant and dose-dependent anti-androgenic activities by two *in vitro* assays (Table 3, Fig. 2, 3). IC_{50} values of them were 3, 28, and 55 μm in the Yeast Two-hybrid assay and 5, 17 and 12 μm in the AR-EcoScreen cell reporter gene assay, whereas IC_{50} of F was 5 and 0.2 μm, respectively (Table 4). Thus anti-androgenic activity of NDBzA was thought to be near F, whereas that of NDPA and NDCHA was about 10 times lower than these compounds.

Mode of Action of NDBzA, NDPA and NDCHA

Many anti-androgens inhibited androgenic action by competition on binding to AR. As shown in Fig. 4, NDBzA, NDPA and NDCHA showed the binding affinity to AR by the competitive binding assay using fluorescent labeling AR ligand. IC_{50} values of NDBzA, NDPA, NDCHA, F and DHT were 20, 183, 27, 29 and 0.04 *m*m, respectively (Table 4). And the binding affinity of NDBzA and NDCHA was estimated to be similar to F, and NDPA was about 10 times lower, although these affinities were 1000 to 10000 times lower than DHT.

The effect of these NOCs on the level of AR protein expression was examined in androgen dependent LNCaP cells. When the cells were treated with DHT for 10 hr, the level of AR increased. Then when LNCaP cells were treated with NDBzA, NDPA, NDCHA and F in the presence of DHT, they decreased the level of AR induced with DHT (Fig. 5). These results suggest that NDBzA, NDPA and NDCHA prevented the DHT induced AR level to inhibit the androgenic action of DHT and another pathway.

Northern blot analysis was applied to determine effect of NOCs on the expression of an endogenous androgen responsive gene in LNCaP cells. The level

Table 3. Effect of NOCs on Luciferase Activity

Compound	Relative β-galactosidase activity (%)	Relative luciferase activity[a)] (%)	Source
N-Nitrosodimethylamine	95.7 ± 4.2	105.1 ± 13.9	Wako
N-Nitrosodiethylamine	103.6 ± 3.1	105.8 ± 9.5	Wako
N-Nitrosodipropylamine	108.3 ± 2.4	94.4 ± 9.1	SUPELCO
N-Nitrosodibutylamine	103.6 ± 2.9	95.8 ± 10.5	SIGMA
N-Nitrosodiisobutylamine	106.4 ± 1.7	95.3 ± 6.0	Wako
N-Nitrosomethylbutylamine	102.1 ± 4.5	102.8 ± 5.7	SIGMA
N-Nitrosoethylbutylamine	101.0 ± 2.9	99.5 ± 8.1	SIGMA
N-Nitrosodiethanolamine	113.4 ± 5.6	98.0 ± 8.4	SIGMA
N-Nitrosodiisopropanolamine	109.5 ± 2.8	91.7 ± 5.1	SIGMA
N-Nitrosodicyclohexylamine	50.7 ± 8.9**	54.2 ± 3.3**	SIGMA-ALDRICH
N-Nitrosodiphenylamine	54.4 ± 5.1**	43.7 ± 1.6**	Wako
N-Nitrosodibenzylamine	51.6 ± 7.7**	3.8 ± 2.5**	SIGMA-ALDRICH
N-Nitrosopiperidine	110.5 ± 2.8	97.0 ± 3.8	SIGMA
N-Nitrosopyrrolidine	114.4 ± 2.2	103.4 ± 8.7	SIGMA-ALDRICH
N-Nitrosomorpholine	109.7 ± 4.2	96.7 ± 8.8	SIGMA

N-Nitroso compound at 10 μm was tested and the relative activity in the presence of 40 nM DHT in the Yeast Two-hybrid assay and 0.5 nM DHT in the AR-EcoScreen cell reporter gene assay were calculated as the percentage against DHT without chemicals (%). Values represent the mean ± S.D. ($n = 3$). **$p < 0.01$ compared to DHT without chemicals.

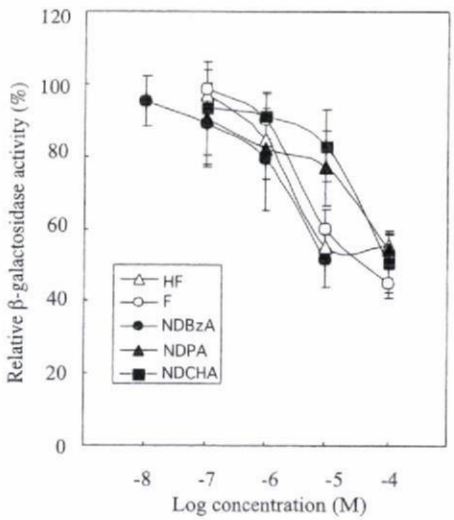

Fig. 2. Dose-Dependent Curves of NOCs in Yeast Two-Hybrid Assay System

Relative β-galactosidase activity of NDBzA, NDPA and NDCHA in the presence of 40 nM DHT was calculated as the percentage against DHT without chemicals (100%). Values represent the mean ± S.D. ($n = 3$).

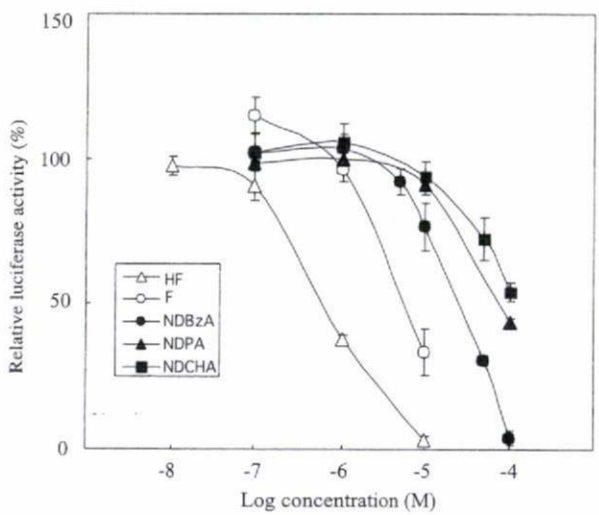

Fig. 3. Dose-Dependent Curves of NOCs in AR-EcoScreen Cell Reporter Gene Assay

Relative luciferase activity of NDBzA, NDPA and NDCHA in the presence of 0.5 nM DHT was calculated as the percentage against DHT without chemicals (100%). Values represent the mean ± S.D. ($n = 3$).

of PSA was about double when the cells were treated with 10 nM DHT for 18 hr, but NDBzA and F decreased the PSA to the same level without DHT. NDPA also decreased the level about 70%, but not NDCHA (Fig. 6).

DISCUSSION

In this study, we assessed the anti-androgenic activity on 56 chemicals using Yeast Two-hybrid assay (AR:SRC-1) and AR-EcoScreen cell reporter gene assay, and found NDPA as a novel anti-androgen. Then we tested on 15 NOCs and found that NDBzA and NDCHA as well as NDPA inhibited the

Table 4. Effects of Compounds on the Inhibition of DHT Activity by the Various Assays

Compounds	Reporter gene assay IC_{50}[a] (μM)	Yeast Two-hybrid assay IC_{50}[a] (μM)	AR binding assay IC_{50}[a] (μM)
F	0.223	4.56	28.6
NDBzA	4.95	2.60	19.9
NDPA	16.9	27.6	183
NDCHA	11.7	54.8	27.4

a) IC_{50} denotes the concentration that chemicals inhibited 50% of DHT without chemicals as described under method.

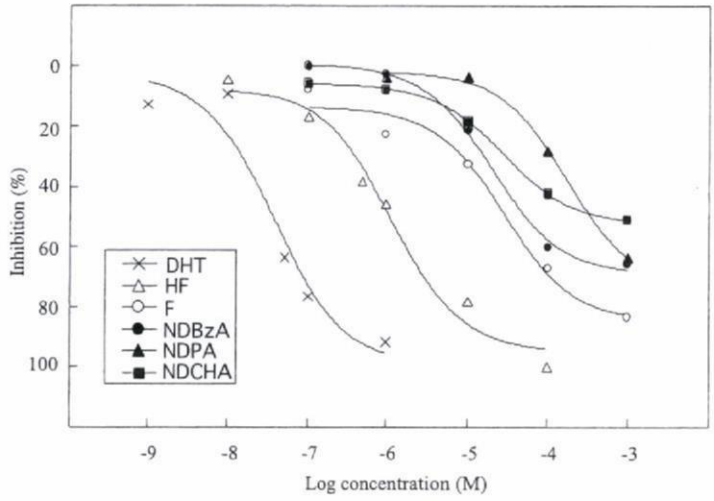

Fig. 4. Competitive Binding of NDBzA, NDPA and NDCHA against AR/AR-Ligand Complex to AR

NDBzA, NDPA and NDCHA competed against Fluormone AL green (fluorescent labeling AR lignads) on binding to human AR. Values represent the mean ± S.D. (n = 3).

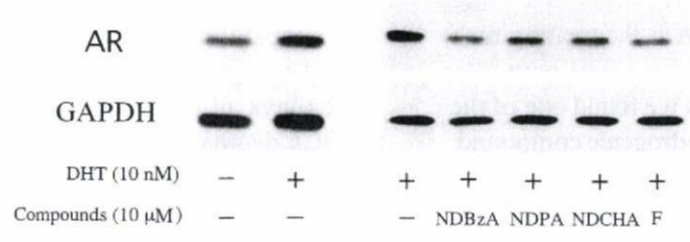

Fig. 5. Effect of NDBzA, NDPA and NDCHA on the Protein Level of AR

LNCaP cells were treated with NDBzA, NDPA and NDCHA in the presence of 10 nM DHT for 10 hr. The level of AR was detected by Western blot analysis.

androgenic activity of DHT.

To estimate the anti-androgenic activity in the Yeast Two-hybrid assay required simpler technique and shorter time, however the sensitivity was lower than the reporter gene assay. Therefore we tested all of the 56 chemicals for anti-androgenic activity by the two *in vitro* assays. Then 9 chemicals found as positive compounds by both. On the other hand, 3 chemicals were positive only by Yeast Two-hybrid assay. The different judgment may be due to difference of used cofactors. Androgen directly interacts with AR, and the complex stimulates transactivation of target genes through interaction with cofactors such as SRC-1, transcription intermediary factor (TIF2), and amplified in breast cancer (AIB1).[23] The AR-EcoScreen cells contain all cofactors, but yeast cells do SRC-1 alone. Another cause may be difference in cell membrane permeability between two

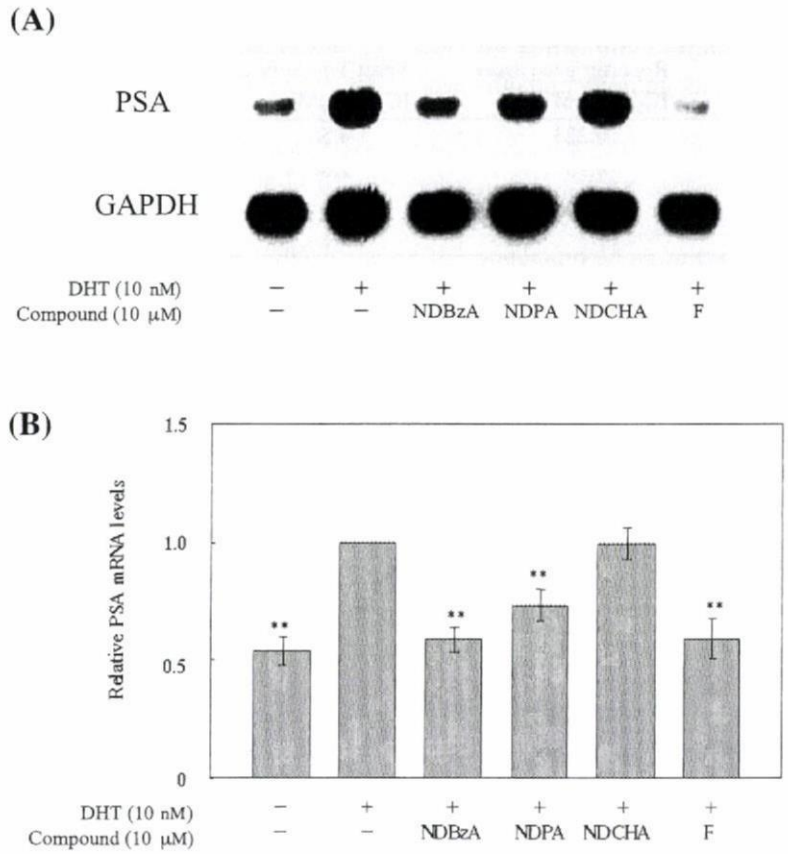

Fig. 6. Effect of NDBzA, NDPA and NDCHA on the Expression of AR Target Gene, PSA

(A) The PSA mRNA levels were determined by Northern blot analysis. LNCaP cells were treated with NOCs in the presence of 10 nM DHT for 18 hr. Total RNA fractions (12 μg each) were subjected to Northern blots. (B) The value of each PSA mRNA level was rectified with the GAPDH. Relative PSA mRNA levels were compared to 10 nM DHT without chemicals (relative PSA mRNA level = 1). Values represent the mean ± S.D. ($n = 3$). $^{**}p < 0.01$ compared to 10 nM DHT without chemicals.

cells and in assay condition such as the treating time of compounds.

Among positive compounds we found one of the NOCs, NDPA, as a novel anti-androgenic compound. Therefore we measured anti-androgenic activity of 15 NOCs to determine whether or not *N*-nitroso group correlated with anti-androgenic activity. As a result NDBzA and NDCHA were positive as well as NDPA, but the others were not. These positive compounds had ring structure other than *N*-nitroso groups. Anti-androgenic activity of NDBzA was estimated the highest, as much as F. NDPA was considered to be higher than NDCHA. These 3 NOCs were competitive in the binding to AR, although binding affinities were low. If the anti-androgenic activity and binding affinity were compared, there is likely to be no correlativity. Because anti-androgenic activity of NDPA was higher than NDCHA, whereas binding affinity of NDPA was less than NDCHA. These results suggest that NDBzA, NDPA and NDCHA antagonized with DHT on the process of competitive binding to AR.

Androgens increase the level of AR protein and AR plays an important role in the nucleus. These NOCs decreased the level of AR, suggesting that NDBzA, NDPA and NDCHA inhibited the androgenic action. The expression of PSA, AR target gene, is regulated by the AR and is thought to function as a growth factor in LNCaP cells.[24–26] Northern blot showed that NDBzA and NDPA inhibited transcriptional level of PSA in LNCaP cells. The same results were obtained by RT-PCR (data not shown). NDBzA inhibited the level of PSA as much as F and NDPA also decreased. These results suggest that 3 NOCs down-regulate the AR target genes mRNA level by antagonizing against DHT in binding process to AR.

This study shows first the anti-androgenic activity of NDBzA, NDPA and NDCHA, that some NOCs may affect endocrine system of humans and wildlife. Thus there are still anti-androgenic compounds that nobody knows. From now on, when we

perform risk assessment of chemicals, it is need to test the androgenic and anti-androgenic effect on endocrine system as well as carcinogenicity and others.

Acknowledgements We thank Drs. M. Kawase at Osaka University and S. Osada at Nagoya City University for their valuable discussion and advice during this study, and also Dr. Yong K. Oh in U.S.A. for checking the English of this manuscript.

REFERENCES

1) Mangelsdorf, H., Thummel, C., Beato, M., Herrlich, P., Schutz, G., Umesono, K., Blumberg, B., Kastner, P., Mark, M. and Chambon, P. (1995) The nuclear receptor superfamily: the second decade. *Cell*, **83**, 835–839.
2) Beato, M., Herrlich, P. and Schutz, G. (1995) Steroid hormone receptors: many actors in search of plot. *Cell*, **83**, 851–857.
3) Cleutjens, K. B., van Eekelen C. C., van der Korput H. A., Brinkmann A. O. and Trapman, J. (1995) Two androgen respose regions cooperate in steroid hormone regulated activity of the prostate-specific antigen promorter. *J. Biol. Chem.*, **271**, 6379–6388.
4) Gobinet, J., Ppujol, N. and Sultan, C. (2002) Molecular action of androgens. *Mol. Cell. Endocrinol.*, **198**, 15–24.
5) Oesterling, J. E. (1991) Prostate specific antigen: a critical assessment of the most useful tumor marker for adenocarcinoma of the prostate. *J. Urol.*, **145**, 907–923.
6) Colborn, T., Dumanoski, D. and Myers, J. P. (1996) *Our stolen future*, Dutton, New York.
7) Nishihara, T., Nishikawa, J., Kanayama, T., Dakeyama, F., Saito, K., Imagawa, M., Takatori, S., Kitagawa, Y., Hori, S. and Utsumi, H. (2000) Estrogenic activities of 517 chemicals by yeast two-hybrid assay. *J. Health Sci.*, **46**, 282–298.
8) Blair, R. M., Fang, H., Branham, W. S., Hass, B. S., Dial, S. L., Moland, C. L., Tong, W., Shi, L., Perkins, R. and Sheehan, D. M. (2000) The estrogen receptor relative binding affinities of 188 natural and xenochemicals: structural diversity of ligands. *Toxicol. Sci.*, **54**, 138–153.
9) Sultan, C., Balaguer, P., Terouanne, B., Georget, V., Paris, F., Jeandel, C., Lumbroso, S. and Nicolas, J. (2001) Environmental xenoestrogens, antiandrogens and disorders of male sexual differentiation. *Mol. Cell. Endocrinol.*, **178**, 99–105.
10) Kojima, H., Katsura. E., Takeichi, S., Niiyama, K. and Kobayashi, K. (2004) Screening for estrogen and androgen receptor activities in 200 pepsticides by *in vitro* receptor gene assays using chinese hamster ovary cells. *Environ. Health Perspect.*, **112**, 524–531.
11) Kelce, W. R., Monosson, E., Gamcsik, M. P., Laws, S. C. and Gray, L. E. (1994) Environmental hormone disruptors: evidence that vinclozolin development toxicity is mediated by antiandrogenic metabolites. *Toxicol. Appl. Pharmcol.*, **126**, 276–285.
12) Kelce, W. R., Stone, C. R., Laws, S. C., Gray, L. E., Kemppainen, J. A. and Wilson, E. M. (1995) Persistent DDT metabolite p,p'-DDE is a potent androgen receptor antagonist. *Nature* (London), **375**, 581–585.
13) Gray, L. E., Ostby, J. S. and Kelce, W. R. (1994) Developmental effects of an environmental antiandrogen: the fungicide vinclozolin alters sex differentiation of the male rat. *Toxicol. Appl. Pharmacol.*, **129**, 46–52.
14) Gray, L. E., Wolf, C., Lambright, C., Mann, P., Cooper, R. L. and Ostby, J. (1999) Administration of potentially antiandrogenic pesticides (procymidone, linuron, iprodione, chlozolinete, p,p'-DDE, and ketoconazol) and toxic substances (dibutyl-and diethylhexyl phthalate, PCB 169, and ethane dimethane sulphonate) during sexual differentiation produces diverse profiles of reproductive malformations in the male rat. *Toxicol. Ind. Health*, **15**, 94–118.
15) Monosson, E., Kelce, W. R., Lambright, C., Ostby, J. and Gray, L. E. (1999) Peripubertal exporsure to the antiandrogenic fungicide, vinclozolin, delays puberty, inhibits the development of androgen-dependent tissues, and alters androgen receptor function in the male rat. *Toxicol. Ind. Health*, **15**, 65–79.
16) Lambright, C., Ostby, J., Bobseine, K., Wilson, V., Hotchkiss, A. K., Mann, P. C. and Gray, E. (2000) Cellular and molecular mechanisms of action of linuron: an antiandrogenic herbicide that produces reproductive malformations in male rats. *Toxicol. Sci.*, **56**, 389–399.
17) Akaza, H., Usami, M., Kotake, T., Koiso, K. and Aso, Y. (1993) A randomized phase II traial of flutamide vs chloromadinone acetate in previously untreated advanced cancer. The Japan Flutamide Study Group. *Jpn. J. Clin. Oncol.*, **23**, 178–185.
18) Lijinsky, W. (1987) Carcinogenecity and mutagenecity of *N*-nitroso compounds. *Mol. Toxicol.*, **1**, 107–119.
19) Mirvish, S. S. (1995) Role of *N*-nitroso compounds (NOC) and *N*-nitrosation in ethiology of gastric, esophageal, nasopharyngeal and bladder cancer and contribution to cancer of known exporsures to NOC. *Cancer Lett.*, **93**, 17–48.
20) Tricker, A. R., Spiegelhalder, B. and Preussmann,

R. (1989) Environmental exporsure to performed nitroso compounds. *Cancer Surv.*, **8**, 251–272.

21) Nishikawa, J., Saito, K., Goto, J., Dakeyama, F., Matsuo, M. and Nishihara, T. (1999) New screening methods for chemicals with hormonal activities using interaction of nuclear hormone receptor with coactivator. *Toxicol. Appl. Pharmcol.*, **154**, 76–83.

22) Satoh, K., Ohyama, K., Aoki, N., Iida, M. and Nagai, F. (2004) Study on anti-androgenic effects of bisphenol a diglycidyl ether (BADGE), bisphenol F diglycidyl ether (BFDGE) and their derivatives using cells stably transfected with human androgen receptor, AR-EcoScreen. *Food Chem. Toxicol.*, **42**, 983–993.

23) Torchiba, J., Rose, D. W., Inostroza, J., Kamei, Y., Westin, S., Glass, C. K. and Rosenfeld, M. G. (1997) The transcriptional coactivater p/CIP binds CBP and mediates nuclear-receptor function. *Nature* (London), **387**, 677–684.

24) Henttu, P. and Vihko, P. (1993) Growth factor regulation of gene expression in the human prostatic carcinoma cell line LNCaP. *Cancer Res.*, **53**, 1051–1058.

25) Lee, C., Sutkowski, D. M., Sensibar, J. A., Zelner, D., Kim, I., Amsel, I., Shaw, N., Prins, G. S. and Kozlowski, J. M. (1995) Regulation of proliferation and production of prostate-specific antigen in androgen-sensitive prostatic cancer cells, LNCaP, by Dihydrotestosterone. *Endocrinology*, **136**, 796–803.

26) Dioxin, S. C., Knopf, K. B. and Figg, W. D. (2001) The control pf prostate-specific antigen expression and gene regulation by pharmacological agents. *Pharmacol. Rev.*, **53**, 73–91.